International Journal of Chemical, Materials and Biomolecular Sciences
ISSN: 2415-6620
Vol:11, No:12, 2017

Modeling Nanomechanical Behavior of ZnO Nanowires as a Function of Nano-Diameter

L. Achou, A. Doghmane

***Abstract*—**Elastic performances, as an essential property of nanowires (NWs), play a significant role in the design and fabrication of modern nanodevices. In this paper, our interest is focused on ZnO NWs to investigate wire diameter ($D_{wire} \leq 400$ nm) effects on elastic properties. The plotted data reveal that a strong size dependence of the elastic constants exists when the wire diameter is smaller than ~ 100 nm. For larger diameters ($D_{wire} > 100$ nm), these ones approach their corresponding bulk values. To enrich this study, we make use of the scanning acoustic microscopy simulation technique. The calculation methodology consists of several steps: determination of longitudinal and transverse wave velocities, calculation of refection coefficients, calculation of acoustic signatures and Rayleigh velocity determination. Quantitatively, it was found that changes in ZnO diameters over the ranges 1 nm $\leq D_{wire} \leq$ 100 nm lead to similar exponential variations, for all elastic parameters, of the from: $A = a + b \exp(-D_{wire}/c)$ where a, b, and c are characteristic constants of a given parameter. The developed relation can be used to predict elastic properties of such NW by just knowing its diameter and vice versa.

***Keywords*—**Elastic properties, nanowires, semiconductors, ZnO.

I. Introduction

ZnO NWs with unique properties intrinsically associated with low dimensionality, size confinement, and large surface area to volume ratio are very promising for applications in electronic, optoelectronic, and sensor devices on a nanometer scale that are characterized by good operation, low power consumption, and high performance [1]-[3]. The analysis of the Young's modulus, E, of ZnO NWs is of great interest for many reasons. Firstly, the Young's modulus is the key material property reflecting the NW's elasticity. Secondly, it is one of the intrinsic parameters of each material: in macroscopic systems, it is constant (140 GPa) [4], but at the nanometer scale, it depends on the nano-diameter. Finally, the determination of the Young's modulus leads to the determination of other elastic parameters such as the shear modulus, bulk modulus, and surface acoustic wave (SAW) velocities.

Depending on the size of objects and the type of mechanical property studied, various theoretical methods and experimental techniques (under different loading modes) have been developed to investigate the nanomechanical behavior [5]. In spite of this great deal of interest, there is neither a theoretical equation nor a single model to predict the relation between size and elastic parameters in ZnO NWs.

In this context, the nano-diameter dependence of the elastic properties of ZnO NWs oriented along the [0001] direction is studied. We first consider the commonly used mechanical characterization methods for measurement/calculation of the Young's modulus of NWs (with $D_{wire} \leq 400$ nm). Then, we investigate the NWs by scanning acoustic microscopy (SAM) technique [6], [7] based on the emission and reflection of SAWs to determine the effects of D_{wire} on acoustic velocities. We also calculate reflection coefficients and acoustic signatures for ZnO NWS. Finally, an expression relating diameter to such acoustic parameters is suggested.

II. Computational Approach

The procedure consists of the following steps:

(a) Data choice: Survey, select and exploit the Young's modulus data measured/calculated by the frequently used experimental/theoretical methods reported in the literature [3], [5], [8]-[11];

(b) Quantification of wire diameter effects on Young's modulus: Plot the data as a function of Dwire (with 1 nm $\leq$ Dwire $\leq$ 400 nm) and then determine an analytical relation E = f(Dwire) in the initial region where the size effects are very important;

(c) Determination of other elastic parameters: Evaluate the diameter effects on the following elastic parameters: shear modulus, G, bulk modulus, B, Poisson's ratio, υ, longitudinal wave velocities, VL, and transverse wave velocities, VT.

These parameters are determined from the combination of the following relations [12], [13]:

$$E/G = 2.587 \quad (1)$$

$$G = \rho V_T^2 \quad (2)$$

$$E = G\,(3V_L^2 - 4V_T^2)/(V_L^2 - V_T^2) = \rho V_T^2 (3V_L^2 - 4V_T^2)/(V_L^2 - V_T^2) \quad (3)$$

$$B = \rho\,(V_L^2 - 3/4\,V_T^2) \quad (4)$$

$$\upsilon = E/2\,(\rho\,V_T^2) - 1 \quad (5)$$

where ρ is the density of bulk ZnO ($\rho_{ZnO} = 5605$ kg/m^3 [14]).

(d) Acoustic Microscopy Computing Procedure: SAM, a non-destructive technique, is based on the determination of acoustic signatures, known as V(z), which are the most important quantitative quantity, can be measured experimentally by recording the output voltage, V, at the piezoelectric transducer when the distance z between the

L. Achou is with the Département de Physique, Faculté des Sciences, Université Badji-Mokhtar, Annaba, BP 12, DZ-23000, Algeria (e-mail: linda_achou@yahoo.fr).

A. Doghmane is with the Laboratoire des Semi-conducteurs, Département de Physique, Faculté des Sciences, Université Badji-Mokhtar, Annaba, BP 12, DZ-23000, Algeria.

lens and the sample surface varies or computed via different corresponding physical models [6], [7], [15]. The computing procedure, for every NW, consists of several steps:

(i) Introducing the above deduced velocities (V_L and V_T) into a simulation program under conventional conditions of a SAM: a lens half-opening angle of 50°, a frequency of 142 MHz, and a Freon couplant with V_{liq} = 716 m/s and ρ_{liq} = 1.57 g/cm^3.

(ii) Calculating reflection coefficients, R(θ), for every liquid/ZnO NW combination, where R(θ) is a complex function admitting a modulus $|R|$ and a phase ϕ, given by [16]-[18]:

$$R(\theta) = (Z_{sol} - Z_{liq})/(Z_{sol} + Z_{liq}) \quad (6)$$

with liquid impedance: $Z_{liq} = \rho_{liq} . V_{liq}/\cos\theta$ (where ρ_{liq} and V_{liq} are the velocity and the density in the coupling liquid, respectively) and solid impedance: $Z_{sol} = Z_L \cos^2(2\theta_L) + Z_T \sin^2(2\theta_T)$ (where Z_L, Z_T are the longitudinal and transverse impedances and θ_L, θ_T are the longitudinal and transverse critical angles).

(iii) Deducing of V(z) curves from:

$$V(z) = \int P^2(\theta) R(\theta) \exp(2jk_o z\cos\theta) \sin\theta\cos\theta d\theta \quad (7)$$

where $P^2(\theta)$ is the pupil function, θ is the half-opening angle of the lens, z is the defocusing distance, and $k_o = 2\pi/\lambda$ is the wave number in the coupling liquid, $j=\sqrt{-1}$.

(iv) Applying fast Fourier transform (FFT) to the treatment of periodic V(z) to deduce Rayleigh velocity, V_R, from the principal peaks of FFT spectra according to [16]:

$$V_R = V_{liq}/\sqrt{1-(1-V_{liq}/2f\Delta Z)^2} \quad (8)$$

where, *f* is the operating frequency.

(e) Determination of A=f(D_{wire}) expression: The A-D_{wire} relation is determined with A representing (E, G, B, V_L, V_T, V_R, θ_L, θ_T, θ_R).

III. Results and Discussion

A. Influence of ZnO NW Diameters on Young's Modulus

To quantify the nanomechanical behavior of ZnO NWs (with $D_{wire} \leq 400$ nm) oriented along the [0001] direction, we consider some data reported by different theoretical and experimental methods under different loading modes (tension, buckling, and resonance). The obtained results are shown in Fig. 1, where the Young's modulus (E) is presented as a function of the diameter (D_{wire}).

Different used methods are classified by the following: (i) computational Molecular Dynamics method (MD) via empirical Buckingham-type potential with Tension loading mode [3], [8] and (ii) experimental methods of Micromechanical system (MEMS) with Tension [3], Contact resonance Atomic Force Microscopy (CR-AFM) [9], Nanoindentation-Transmission Electron Microscopy (NI-TEM) [5], Scanning Electron Microscopy (SEM) with Tension [10], SEM with Buckling [10], and AFM Cantilever in situ SEM with Tension [11]. The horizontal dashed line represents the corresponding bulk value along the [0001] direction [4].

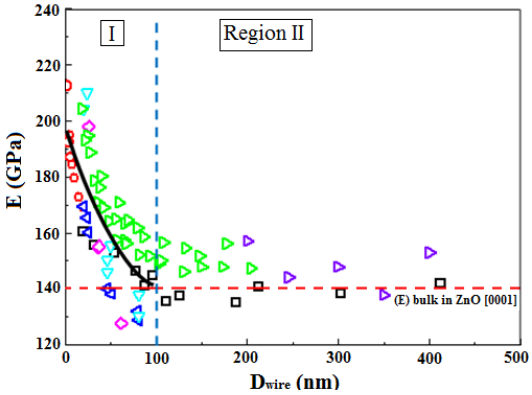

Fig. 1 Influence of ZnO NW diameters (D_{wire}) on Young's modulus using (i) computational MD method: Tension (○) [3], [8] and (ii) experimental methods: MEMS system (□): Tension [3], CR-AFM (◇) [9], NI-TEM (▷) [5], SEM: Tension (◁) [10], SEM: Buckling (▽) [10], AFM Cantilever in situ SEM: Tension (▷) [11]. The horizontal dashed line represents the bulk value along the [0001] direction [4]; the continuous line (—) represents the best fit in the initial region

It is clear that the general trend of the E-D_{wire} curves obtained by all methods is characterized by a rapid initial decrease for small diameters ($D_{wire} \leq 100$ nm) followed by a tendency towards saturation for higher diameters (100 nm ≤ D_{wire} ≤ 400 nm). The E-D_{wire} behavior in initial decreasing region can be expressed by an exponential dependence obtained via curve fitting (plotted as solid line):

$$E = 127 + 75.37 \exp(-D_{wire}/58.38) \quad (9)$$

We notice that the mechanical behavior of ZnO changes from that of NWs to bulk material at the critical diameter ($D_{wire} \approx 100$ nm) for which ($E_{wire} \approx E_{bulk} = 140$ GPa).

B. Influence of ZnO NW Diameters on Elastic Parameters

TABLE I
Elastic Constants and Wave Velocities Are Calculated in Both NWs and Bulk ZnO

D_{wire} (nm)	Calculated					
	E (GPa)	G (GPa)	υ	B (GPa)	V_L (m/s)	V_T (m/s)
1	201.09	77.73	0.29	162.31	6888	3724
10	190.50	73.64	0.29	153.72	6704	3625
20	180.51	69.78	0.29	145.64	6526	3528
30	172.08	66.52	0.29	138.85	6372	3445
40	164.99	63.78	0.29	133.12	6239	3373
50	159.00	61.46	0.29	128.34	6125	3311
60	153.97	59.52	0.29	124.23	6027	3259
70	149.72	57.87	0.29	120.89	5944	3213
80	146.15	56.49	0.29	118.01	5873	3175
90	143.13	55.33	0.29	115.48	5811	3142
100	140.59	54.34	0.29	113.53	5760	3114
Bulk	140.00	54.12	0.29	112.95	5747	3107

To study the influence of nano-diameters on elastic constants and wave velocities (E, G, B, ν, V_L, and V_T) of ZnO NWs, we must focus on the previously deduced relation (9) as well as (1)-(5). Several D_{wire} values were chosen from 1 to 100 nm with a step of 10. The results, thus obtained, are shown in Table I.

It is clear that, whenever the wire diameters increase, the elastic parameters decrease till they reach bulk values, confirming the dependence of elastic properties with the size for $D_{wire} \leq 100$ nm.

C. Influence of ZnO NW Diameters on R(θ) and V(z) Curves

To illustrate the influence of ZnO wire diameter on reflection coefficient and acoustic signatures, we plot in Fig. 2 typical results (D_{wire} = 10 nm, 30 nm, 50 nm, 70 nm, and 90 nm) of the variation of R(θ) in terms of amplitude (dashed line referred to the left hand side) and phase (solid line referred to the right-hand side) as a function of incident angles, θi (Fig. 2 (a)) and V(z) curves with FFT spectra (Fig. 2 (b)). It is obvious that:

(i) For all NWs, the amplitude of R(θ) curves (Fig. 2 (a)) has similar behavior (a saturation, a sharp peak, another saturation, a smooth increase and a final saturation with $|R| = 1$). The first fluctuation corresponds to the excitation longitudinal waves at critical angles, θ_L and the second in amplitude corresponds to the excitation transverse waves at critical angles, θ_T.
(ii) The displacement of critical angles (θ_L and θ_T) gradually becomes high when D_{wire} increases from 10 to 90 nm.
(iii) All the curves dealing with the phase show a large fluctuation of 2π around the Rayleigh-wave critical angle, θ_R. The θ_R fluctuations increase from 12.50° to 14.60° as the diameters increase from 10 to 90 nm.
(iv) All the acoustic signatures curves, in Fig. 2 (b), exhibit a series of regular periodical oscillations, Δ(*z*), between two successive maxima or minima. These oscillations are due to the interference between two acoustical components detected by the transducer [6], [7], [16].
(i) As D_{wire} increases, we notice a change in V(z) amplitudes as well as in Δ(*z*).
(ii) The spectral analysis of V(z) curves is carried out via FFT treatment. The periods Δz are closely related to the SAW velocities of the material studied. Hence, each principal ray corresponds to the velocity of a given mode [6], [7], [16]. The analysis of the FFT spectra confirms the decreasing of velocity of longitudinal and Rayleigh modes with increasing D_{wire}. As D_{wire} change from 10 to 90 nm, V_L decreases from 6704 to 5811 m/s and V_R from 3371 to 2922 m/s.
(iii) At D_{wire} = 90 nm, the critical angles (θ_L, θ_T, θ_R), the V(z) signatures, and the wave velocities (V_L, V_R) of NWs approach the values of their analogous bulk values.

D. Quantification of Nanomechanical Behavior

To enhance the present work and validate the above results that were obtained from E-D_{wire} (9), we plot the calculated results of shear modulus, G, bulk modulus, B, and velocities: V_L, V_T, and V_R at different values of D_{wire}. Some typical results are depicted in Fig. 3. The general tendency is for a decrease in G, B, V_L, V_T, and V_R as ZnO wire diameters increase. Using a simple fitting procedure, it is possible to find exponential dependence (black solid line) of the form:

$$G = 49.08+29.15 \exp(-D_{wire}/58.43) \quad (10)$$

$$B = 102.69+60.64 \exp(-D_{wire}/58.04) \quad (11)$$

$$V_L = 5437.97+1473.84 \exp(-D_{wire}/65.57) \quad (12)$$

$$V_T = 2937.83+798.96 \exp(-D_{wire}/65.88) \quad (13)$$

$$V_R = 2732.63+742.91 \exp(-D_{wire}/65.85) \quad (14)$$

All these relations of similar exponential forms can be expressed as:

$$A = a + b \exp(-D_{wire}/c) \quad (15)$$

where a, b, and c are the characteristic constants deduced for each parameter; the values of these constants are regrouped in Table II.

The advantage of the present equation lies in the possibility of evaluating the elastic properties based on the NW diameter (as shown in our previous works [13], [19], [20]). This would be useful for experimental synthesis and technological applications by designing such ZnO wire with desired properties to achieve the adequate elasticity which is highly required for good reliability and high performance of nanoscale devices.

It is worth noting that the ZnO NWs are likely to behave as bulk ZnO for $D_{wire} \geq 100$ nm whose E = 140 GPa, G = 54.12 GPa, B = 112.95 GPa, V_L = 5747 m/s, V_T = 3107 m/s and V_R = 2890 m/s.

TABLE II
DEDUCED CHARACTERISTIC CONSTANT VALUES IN THE RELATIONSHIP A=A+B EXP(-D_{WIRE}/C) FOR ALL ACOUSTIC PARAMETERS WHERE A REPRESENT (E, G, B, V_L, V_T, V_R, Θ_L, Θ_T, Θ_R)

Const.	E	G	B	V_L	V_T	V_R	θ_L	θ_T	θ_R
a	127	49.08	102.69	5437.97	2937.83	2732.63	8.19	15.14	16.12
b	75.37	29.15	60.64	1473.84	798.96	742.91	-1.96	-3.58	-4.01
c	58.38	58.43	58.04	65.57	65.88	65.85	95.94	91.32	103.11

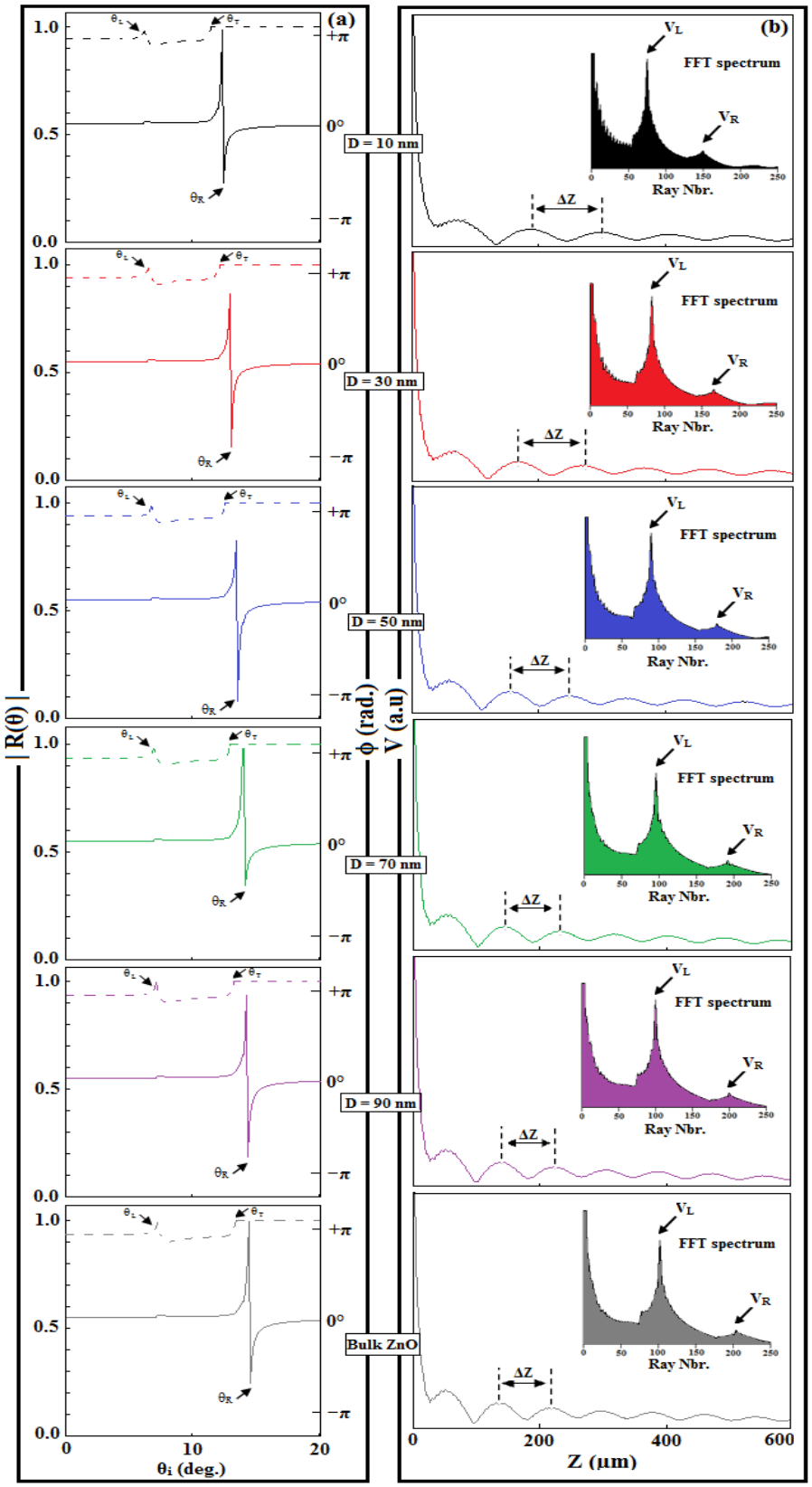

Fig. 2 Effects of ZnO wire diameters, 1 nm ≤ D_{wire}≤ 90 nm, on (a) R(θ) modulus (dashed line) and phase (solid line) and (b) V(z) with their FFT spectra. The lowest curves represent those of bulk ZnO, for comparison

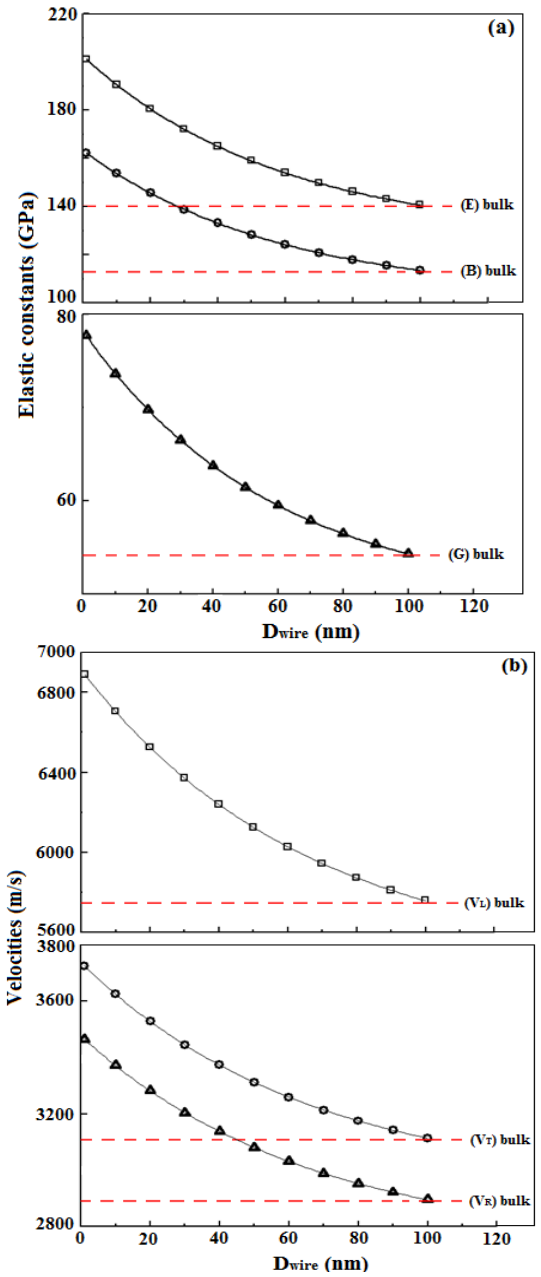

Fig. 3 Effects of ZnO wire diameters (D_{wire}) on (a) elastic constants: E (□), B (○) and G (Δ) and (b) velocities: V_L (□), V_T (○) and V_R (Δ). The horizontal dashed lines represent the corresponding calculated bulk value along the [0001] direction

IV. Conclusion

The effects of ZnO NWs diameters ($D_{wire} \leq 400$ nm) on Young's modulus have been investigated and extended to other acoustic parameters. It was found that, for increasing wire diameters, all the curves show two distinct behaviors: an initial decrease followed by a saturation region that begins at $D_{wire} = 100$ nm corresponding to bulk materials values. The quantification of the initial decreasing region was found to have an exponential behavior of the form $A = a + b\exp(-D_{wire}/c)$ where a, b, and c are characteristic constants. Thus, the importance of such formula lies in the prediction of elastic-acoustic properties of ZnO NWs through control of wire diameters and vice versa.

References

[1] Y. N. Xia, P. Yang, F. Kim and H. Yan, *Adv. Mater* 15, 353 (2003).
[2] S. Kuchibhatla, A. Karakoti, D. Bera and S. Seal, *Prog. Mater. Science* 52, 699 (2007).
[3] R. Agrawal, B. Peng, E. E. Gdoutos, and H. D. Espinosa, *Nano Letters* 8, 3668–3674 (2008).
[4] G. Simmons and H. Wang, MIT Press, Cambridge, MA, 1971.
[5] A. Asthana, K. Momeni1, A. Prasad, Y. K. Yap and R. S. Yassar, *Nanotechnology* 22, 265712-1–265712-10 (2011).
[6] A. Briggs, "Advances in Acoustic Microscopy", Plenum Press, New York, 1995.
[7] A. Briggs, "Acoustic Microscopy", Clarendon Press, Oxford, 1992.
[8] J. Hu and B. C. Pan, *Appl. Physics* 105, 034302-1–034302-6 (2009).
[9] G. Stan, C. V. Ciobanu, P. M. Parthangal and R. F. Cook, *Nano Letters* 7, 3691-3697 (2007).
[10] F. Xu, Q. Qin, A. Mishra, Y. Gu and Y. Zhu, *Nano Research* 3, 271-280 (2010).
[11] M. R. He, Y. Shi, W. Zhou, J. W. Chen, Y. J. Yan and J. Zhu, *Appl. Phys. Letters* 95, 091912-1–091912-3 (2009).
[12] M. Doghmane, F. Hadjoub, A. Doghmane and Z. Hadjoub, *Mater. Letters* 61, 813–816 (2007).
[13] I. Al-Surayhi, A. Doghmane and Z. Hadjoub, Damage and Fracture Mechanics, edited by T. Boukharouba et al., Berlin: Springer Verlag, 2009, pp. 415–424.
[14] D. R. Lide, CRC Handbook of Chemistry and Physics, 73rd Edition, CRC Press, New York, 1992.
[15] C. G. R. Sheppard and T. Wilson, *Appl. Phys. Letters* 38, 858–859 (1981).
[16] J. Kushibiki and N. Chubachi, IEEE Sonics Ultrason, SU-32, 189–212 (1985).
[17] R. D. Weglein, IEEE Sonics Ultrason, SU-27, 82–86 (1980).
[18] Z. Yu, Rev. Mod. Physics 67, 863–891 (1995).
[19] A. Doghmane, L. Achou and Z. Hadjoub, *Journal of Optoelectronics and Advanced Materials* 18, 685-690 (2016).
[20] L. Achou, "Nanophysique et nanotechnologies: Effets de la basse dimensionnalité sur les paramètres énergétiques et acoustiques de nanomatériaux", *Editions Universitaires Européennes*, ISBN 978-620-2-26540-9.